

Original Research

# Drought Stress Inhibits Starch Accumulation in Taro (*Colocasia esculenta* L. Schott)

Erjin Zhang<sup>1,2,3,†</sup>, Weijie Jiang<sup>1,2,3,†</sup>, Wenlong Li<sup>1,2,3</sup>, Ebenezer Ottopah Ansa<sup>1,2,3</sup>,  
Xunrun Yu<sup>1,2,3</sup>, Yunfei Wu<sup>1,2,3,\*</sup>, Fei Xiong<sup>1,2,3,\*</sup><sup>1</sup>Jiangsu Key Laboratory of Crop Genetics and Physiology, Yangzhou University, 225009 Yangzhou, Jiangsu, China<sup>2</sup>Co-Innovation Center for Modern Production Technology of Grain Crops, Yangzhou University, 225009 Yangzhou, Jiangsu, China<sup>3</sup>Joint International Research Laboratory of Agriculture & Agri-Product Safety, Yangzhou University, 225009 Yangzhou, Jiangsu, China\*Correspondence: [006949@yzu.edu.cn](mailto:006949@yzu.edu.cn) (Yunfei Wu); [feixiong@yzu.edu.cn](mailto:feixiong@yzu.edu.cn) (Fei Xiong)

†These authors contributed equally.

Academic Editor: Naeem Khan

Submitted: 18 July 2023 Revised: 7 October 2023 Accepted: 20 October 2023 Published: 5 February 2024

## Abstract

**Background:** *Colocasia esculenta* L. Schott is a main traditional root crop in China, serving as an important vegetable and staple food. Drought stress plays vital role on the growth and development of taro corm. **Methods:** Two different varieties of taro in Jiangsu were selected: Xiangsha taro and Longxiang taro. The accumulation characteristics, morphological structure, and physicochemical properties of taro corm starch were studied by microscopic observation, particle size analysis, and X-ray diffractometer (XRD) analysis. Transcriptome analyses were used to identify the related genes of taro corm under drought stress. **Results:** During the growth of taro, the number of amyloplasts showed an obvious increasing trend and shifted from being dispersed throughout the cells to being gathered on one side of the cells, and morphological observations showed that smaller granular distribution gradually changed to a larger lumpy distribution. The particle size of Longxiang taro is smaller than that of Xiangsha taro. Under drought stress conditions, the occurrence of starch grains and corm size were inhibited in Xiangsha taro. Transcriptome sequencing of drought-stressed taro corms showed that the enzymes related to starch synthesis were differentially expressed. Kyoto Encyclopedia of Genes and Genomes (KEGG) enrichment analysis of drought-stressed taro corms showed that drought affected hormone signal transduction, material metabolism, drought stress tolerance, plant growth and development, and stress resistance, which triggered the plant drought adaptive response. **Conclusions:** Drought stress inhibits starch accumulation in taro.

**Keywords:** drought stress; starch; gene expression; corm; taro

## 1. Introduction

Taro (*Colocasia esculenta* L. Schott) is considered to be one of the oldest crops. It is a vegetatively propagated tropical root that is dependent on wet and highly irrigated growth conditions. Its production reached 40.09 million tons in 2019 and ranked fifth among root crops [1]. Corm is mainly used as the propagation material of taro, and underground corm is primarily composed of a main large taro and smaller taro. According to corm development morphology, taro can be divided into the following major growth stages: establishment, vegetative period, corm initiation, and bulking through maturity. Starch in taro is mainly composed of amylose and amylopectin, and the ratio determines the physicochemical properties of starch [2–4].

Drought is a major abiotic stress that dramatically limits key physiological and biochemical processes, which further affects plant growth and crop productivity. Drought triggers the excessive generation of reactive oxygen species, affecting redox homeostasis and resulting in oxidative stress as evidenced by a decline in photosynthetic efficiency, severe cellular damage, reduction in cell membrane stability, and increase in protein denaturation,

among others [5–7]. The cell wall acts as the main perception mechanism of abiotic signals, and also has important roles in growth, development, and turgor pressure [8–10]. Plant cell walls are classified into primary and secondary cell walls, which are formed by polysaccharides such as cellulose, xylans, hemicelluloses, pectins, and structural proteins [11–13]. Abiotic conditions cause an increase in cell wall structural components such as receptors, proteins, carbohydrates, and lignin, which may activate sensing and signaling factors, plant defense systems, and intercellular communication, among others [14–16]. Furthermore, drought stress induces the biosynthesis of abscisic acid (ABA), which is essential to help plants adapt and activate drought stress responses [17–19]. The ABA signaling pathway involves three core components: pyrabactin resistance (PYR)/PYR1-like (PYL)/regulatory component of the ABA receptor, negative regulators belonging to the clade A protein phosphatase 2C family, and protein kinases from the sucrose nonfermenting 1-related protein kinase 2 family, whose downstream substrates include key transcription factors (TFs) and ion channels [20–23].



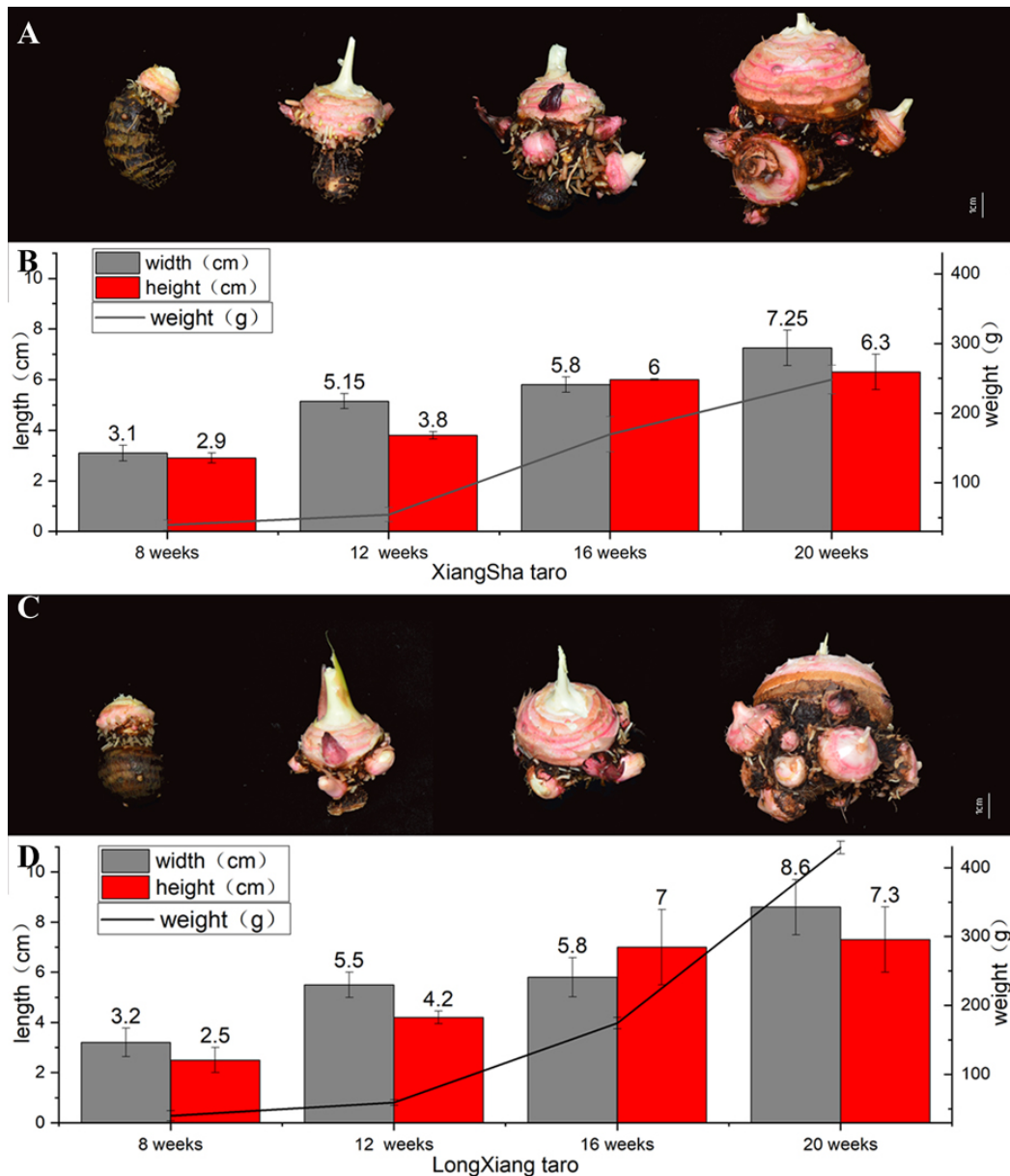


**Fig. 1. Agronomic characters of 'Xiangsha' taro and 'Longxiang' taro in different periods. (A,B) 'Xiangsha' taro. (C,D) 'Longxiang' taro.**

Under drought stress, water use efficiency shows a positive correlation with total plant biomass and a negative correlation with carbon content. Corm nitrogen content is positively correlated with whole-plant level and corm nitrogen content [24]. The magnitude of this loss, however, mostly depends on the duration and severity of drought episodes as well as the plant growth stage and cultivar.

In this study, we analyzed starch accumulation during taro development and its response to drought stress.

## 2. Material and Methods

### 2.1 Plant Materials and Drought Treatment

The taro cultivars of Xiangsha and Longxiang were planted in the experimental field of Yangzhou University

from April 2019 to November 2019. We grew seed taro of Xiangsha taro on April 14, 2019 for 10 weeks in normal conditions, and then with 4 weeks of drought stress. The same-size and disease-free mother taro specimens were selected for the experiment.

### 2.2 Iodine-Potassium Iodide Histochemical Staining

Cross-sections of the taro corms were placed in iodine-potassium iodide ( $I_2$ -KI) solution (1% potassium iodide and 0.3% iodine) in the dark for 10 s at 25 °C, observed, and photographed with the Leica DMLS microscope (Leica Microsystems, Wetzlar, Germany).

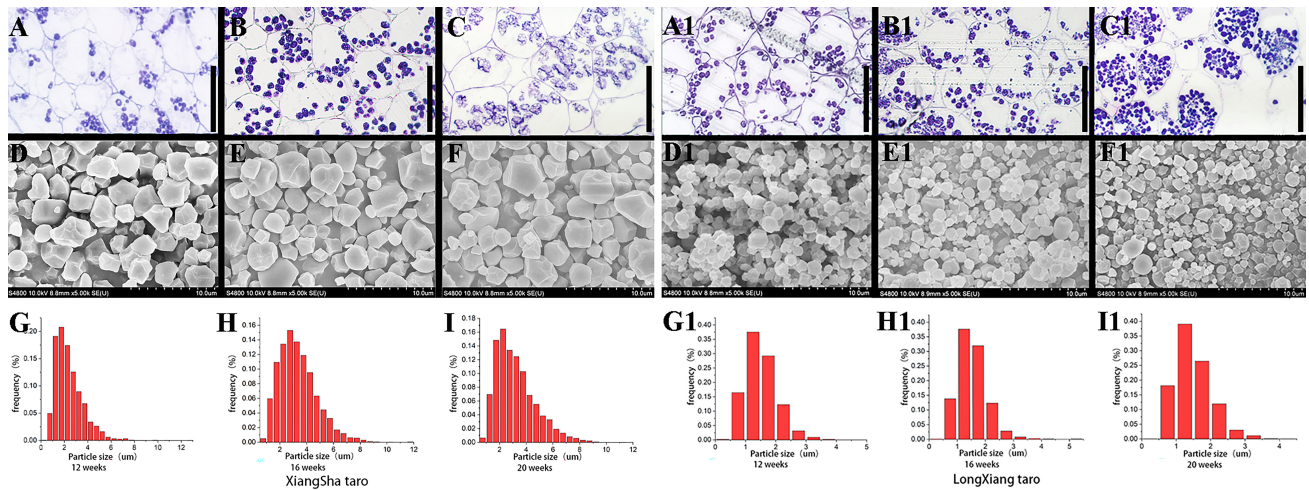


**Fig. 2. Starch characteristics of ‘Longxiang’ taro and ‘Xiangsha’ taro in different periods.** (A–C, A1–C1) Semi thin section staining observation of amyloid; (D–F, D1–F1) starch granules under scanning electron microscope; (G–I, G1–I1) starch particle size distribution map. (A, D, G, A1, D1, G1) Budding period (12 weeks). (B, E, H, B1, E1, H1) Bulb expansion stage (16 weeks). (C, F, I, C1, F1, I1) Maturity (20 weeks). Scale bar: (A–C, A1–C1)—10  $\mu\text{m}$ .

### 2.3 Structural Observation of Taro Corm, Starch Extraction, Morphological Observation, Granule Size Distribution, and X-Ray Diffractometer Analysis

Structural observation of taro corm was conducted and starch was isolated, which was further used for morphological observation, granule size distribution, and X-ray diffractometer (XRD) analysis in accordance with the method described by Yu *et al.* [25]. A small amount of starch was dispersed and spotted on the sample table of a scanning electron microscope. After drying at room temperature, the surface was plated with gold in an etch coater (BAL-TEC SCD 500 Sputter Coater, Leica, Germany). The samples were observed under a field-emission Scanning Electron Microscope (S4800, Hitachi, Tokyo, Japan) and photographed. For the determination of size distribution of starch granules, a small amount of dried starch was transferred to a glass slide, mixed by 50% glycerol, and then covered with a coverslip. Photographs of the freely dispersible sample were captured using an optical microscope (200 $\times$ ). The Image-Pro Plus image analysis software (Image-Pro Plus 7, Media Cybernetics, Rockville, MD, USA) was used to measure starch granule size (maximum axial length of the center of the granule) in the image. Starch granules from each starch sample of the four groups was randomly counted for 1500 times, and the measurement was repeated in triplicate. The starch samples were first absorbed by saturated sodium chloride for 7 days and then compressed with XRD (D8 Advance, Bruker, Mannheim, Germany) to obtain the starch sample XRD pattern.

### 2.4 Transcriptome Analysis

Both drought stress team and control of Xiangsha taro were used for transcriptomic analysis. Total RNA was extracted from the inner tissues of the middle parts, cut into

1-cm-thick square samples of Xiangsha taro. The samples were separated, frozen immediately in liquid nitrogen, and stored at  $-80\text{ }^{\circ}\text{C}$  before RNA isolation. Total RNA was isolated using the Ultrapure RNA Kit (CW0581S; CoWin Biosciences [CW BIO], Cambridge, MA, USA). The mRNA was sent to CW BIO for transcriptome analysis according to the method described by Huang *et al.* [26]. In this study, transcript expression was evaluated, and differentially expressed genes (DEGs) with  $q < 0.05$  and fold change  $> 2$  between the control and treated samples were considered significantly differentially expressed [26]. The functional annotation of DEGs was performed using Gene Ontology (GO) and Kyoto Encyclopedia of Genes and Genomes (KEGG) pathway analysis [26].

### 2.5 Statistical Analyses

The results are represented as the main average of taro plants corms in each of the three control vs three drought individual rows. All samples data were analyzed with Student’s *t*-test using Microsoft Excel 2010 (Microsoft, Redmond, WA, USA) and SPSS software (19.0, IBM Corp., Armonk, NY, USA) to determine any statistically significant differences among the samples. Student’s *t*-test was used to compare means at a significance level of  $p < 0.05$  or  $p < 0.01$ .

## 3. Results

### 3.1 Xiangsha and Longxiang Share Similar Growth Characters in Corm Size

Xiangsha taro and Longxiang taro are two different cultivars of multiseed taros, which were grown in a paddy field 2019 in April in the Jiangsu Province of China. The images of the cultivated taro at 8, 12, 16, and 20 weeks are shown in Fig. 1A,C. Both Xiangsha taro and Longxiang taro

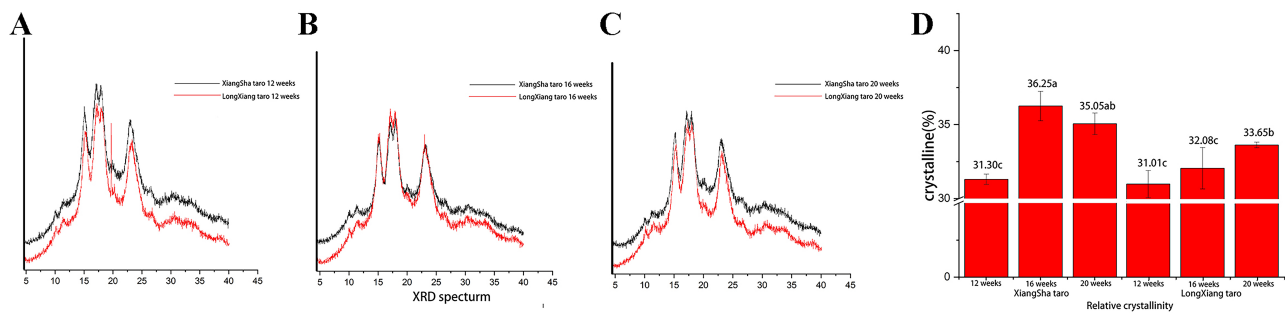


**Fig. 3. X-ray diffractometer (XRD) patterns and relative crystallinity of ‘Xiangsha’ taro and ‘Longxiang’ taro starch grains in different periods.** (A–C) XRD patterns of starch grains. (A) Budding stage. (B) Bulb expansion stage. (C) Maturity period. (D) Relative crystallinity of starch particles.

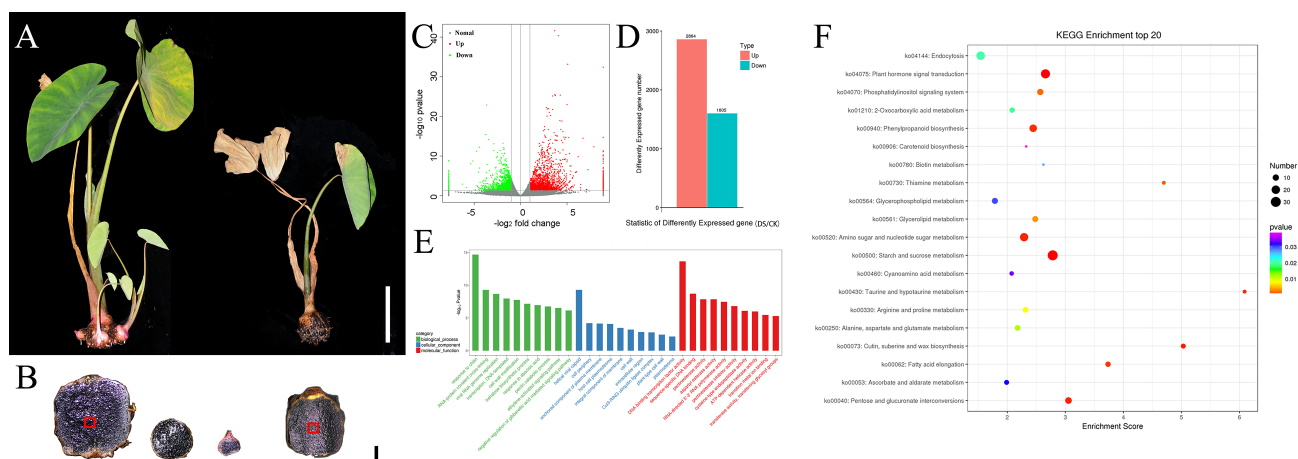


**Fig. 4. Transcriptome sequencing analysis of related genes of ‘Xiangsha’ Taro under drought stress.** (A) Agronomic characters of ‘Xiangsha’ taro after 4 weeks of drought. (B) Bulb iodine staining. (C,D) Transcriptome sequencing data compare with Wild type (WT) and drought stress. (E) Gene Ontology (GO) annotation analysis. (F) Top 20 of Kyoto Encyclopedia of Genes and Genomes (KEGG) pathway enrichment.

were formed at 12 weeks. The height and width of Xiangsha taro were increased to 166.12% and 131.03% at 8 and 12 weeks, respectively (Fig. 1B), whereas the height and width of Longxiang taro were increased to 171.87% and 168%, respectively (Fig. 1D). The width increased faster than height as the seed taro grew at 16 weeks. As growth continued to 20 weeks, there was recovery in the height of the mother taro. The rate of increase in height was faster than that in width. The fastest period of increase in total weight was at 12–16 weeks in Xiangsha taro and 16–20 weeks in Longxiang taro.

### 3.2 Starch Granule Size of Xiangsha Taro Enlarges in the Bulbous Expansion Period

To analyze the difference between Xiangsha taro and Longxiang taro at the starch accumulation level, we used cross-sectioning and  $I_2$  staining. In the vegetative stage of bulb development, the starch bodies in the cells were present as fine granules and distributed on one side of the cells (Fig. 2A,A1). After 4 weeks of development, the

starch bodies increased in volume, but with no obvious changes in location, distribution, or quantity (Fig. 2B,B1). However, in the mature stage of the starch development of taro, the number of starch bodies was significantly increased. The distribution changed from one side of the cell, spreading almost to the entire inner portions of the cell, showing a trend of aggregation in morphology (Fig. 2C,C1). This suggests that both Xiangsha taro and Longxiang taro have similar agronomic characteristics in height, width, and weight during starch accumulation. However, the starch bodies of Xiangsha taro tend to combine into larger granule sizes in the later stage of development, whereas Longxiang taro is still dispersed in cells as multiple small sizes of starch.

To further prove this difference, we analyzed the starch granule size with a scanning electron microscope. Both taro starch granules were polygonal in shape with sharp angles and edges (Fig. 2D–F,D1–F1), but the size of starch in Xiangsha taro was bigger than that in Longxiang taro (Fig. 2G–I,G1–I1). The granule size distribution of

**Table 1. Hormone, wax and secondary messenger related genes under drought stress.**

Gene_id	KEGG gene name	Fold Change	KEGG description
comp9009_c0_seq1	<i>PYL</i>	0.226815124	abscisic acid receptor PYR/PYL family
comp8652_c0_seq1	<i>MYC2</i>	0.464756304	transcription factor MYC2
comp29663_c0_seq1	<i>AHP</i>	4.449523218	histidine-containing phosphotransfer peotein
comp6091_c0_seq2	<i>AHK2_3_4</i>	2.959178847	arabidopsis histidine kinase 2/3/4 (cytokinin receptor)
comp7825_c0_seq1	<i>ARR-A</i>	2.972846249	two-component response regulator ARR-A family
comp26403_c0_seq1	<i>ARR-B</i>	0.338402632	two-component response regulator ARR-B family
comp12872_c0_seq1	<i>JAZ</i>	2.925801272	jasmonate ZIM domain-containing protein
comp11892_c0_seq1	<i>JAZ</i>	2.102210883	jasmonate ZIM domain-containing protein
comp14363_c0_seq1	<i>JAZ</i>	0.266547207	jasmonate ZIM domain-containing protein
comp16857_c0_seq1	<i>ETR, ERS</i>	2.307383882	ethylene receptor
comp18496_c0_seq1	<i>ETR, ERS</i>	2.720212742	ethylene receptor
comp25676_c0_seq1	<i>ETR, ERS</i>	2.685516117	ethylene receptor
comp3157_c0_seq1	<i>ARF</i>	2.130871244	auxin response factor
comp20988_c0_seq1	<i>IAA</i>	5.651279834	auxin-responsive protein IAA
comp31520_c0_seq1	<i>GH3</i>	13.70266474	auxin responsive GH3 gene family
comp13839_c0_seq1	<i>IAA</i>	0.315357539	auxin-responsive protein IAA
comp2650_c0_seq1	<i>CYP86A4S</i>	5.997021747	fatty acid omega-hydroxylase
comp28334_c0_seq1	<i>CYP86A4S</i>	5.444642045	fatty acid omega-hydroxylase
comp26517_c0_seq1	<i>CER1</i>	18.55792524	aldehyde decarboxylase
comp57280_c0_seq1	<i>CER1</i>	5.583134691	aldehyde decarboxylase
comp21117_c0_seq1	<i>CALM</i>	3.960591372	calmodulin
comp24865_c0_seq1	<i>CALM</i>	5.891360704	calmodulin
comp2927_c0_seq2	<i>DGK</i>	4.20089639	diacylglycerol kinase (ATP)
comp20971_c0_seq1	<i>ITPK1</i>	2.288981102	inositol-1,3,4-trisphosphate 5/6-kinase
comp23551_c0_seq1	<i>PIP5K</i>	5.272179139	1-phosphatidylinositol-4-phosphate 5-kinase
comp3524_c0_seq1	<i>PIP5K</i>	2.020090248	1-phosphatidylinositol-4-phosphate 5-kinase

starches in Xiangsha taro peaked at 1–2.5  $\mu\text{m}$  and contained less large-sized starch granules ( $>6 \mu\text{m}$ ) at 12 weeks. The granule size distribution of starches in Xiangsha taro peaked at 2–3.5  $\mu\text{m}$  and 1.5–3  $\mu\text{m}$  at 16 and 20 weeks, respectively, and also contained less large-sized starch granules ( $>6 \mu\text{m}$ ). However, a bigger size ( $>6 \mu\text{m}$ ) of starch granule size at both 16 and 20 weeks was observed. There was no difference in granule size distribution of starches among Longxiang taro at 12, 16, and 20 weeks, and all granule sizes were no more than 4  $\mu\text{m}$  and peaked at 1.25  $\mu\text{m}$ . These data indicated that the increase in starch particle size of Xiangsha taro was greater than that of Longxiang taro during the corm expansion period.

### 3.3 Starch Crystallinity of Xiangsha Taro Transits in the Bulbous Expansion Period

Crystallinity of starch is a parameter that reveals the properties of starch granules, and its numerical changes directly affect the application properties of starch. The starch crystallinity of Longxiang taro basically increased with the growth cycle, whereas the crystallinity of Xiangsha taro was highest in the bulbous expansion period. Even though the crystal structure of taro starch was similar, the relative crystallinity difference between different varieties in different periods was clear. The results of comparisons of dif-

ferent periods were as follows: Xiangsha taro (36.25%) in the bulbous expansion period  $>$  Xiangsha taro (35.05%) in the mature period  $>$  Xiangsha taro (31.30%) in the growing period; Longxiang taro in the mature stage (33.65%)  $>$  Longxiang taro in the bulbous expansion stage (32.08%)  $>$  Longxiang taro in the growing stage (31.01%) (Fig. 3). These data suggested that Xiangsha taro in the bulbous expansion period had a significantly higher transition degree than Longxiang taro.

### 3.4 Transcriptome Analysis Selects Putative Downstream Signaling of Drought Stress

The period of 16 weeks taro is around July to August, which is very hot and short of water. As observed, starch accumulation in Xiangsha taro was more sensitive than that in Longxiang taro. So we chose Xiangsha taro for drought stress analysis. We found that the taro plant growth was higher under normal conditions than under drought stress (Fig. 4A), and there was more seed taro in the control (Fig. 4A). With  $\text{I}_2$ -stained tests, both taros showed bluish purple color. These data demonstrated that drought stress inhibited taro extension and seed taro number.

To investigate drought stress-related genes, we conducted transcriptome analysis using mRNAs prepared from the bulbs of Xiangsha taro in the expansion stage. The

**Table 2. Starch synthesis related genes under drought stress.**

gene_id	KEGG gene name	Fold Change	KEGG description
comp14376_c0_seq1	<i>TPP</i>	3.106661254	trehalose 6-phosphate phosphatase
comp16404_c0_seq1	<i>TPP</i>	15.15949665	trehalose 6-phosphate phosphatase
comp13618_c0_seq1	<i>TPS</i>	3.154252285	trehalose 6-phosphate synthase/phosphatase
comp14277_c0_seq1	<i>TPS</i>	3.150664045	trehalose 6-phosphate synthase/phosphatase
comp17820_c0_seq1	<i>TPS</i>	5.799505188	trehalose 6-phosphate synthase/phosphatase
comp18999_c0_seq1	<i>TPS</i>	5.567555388	trehalose 6-phosphate synthase/phosphatase
comp8937_c0_seq1	<i>TPS</i>	3.718856344	trehalose 6-phosphate synthase/phosphatase
comp11564_c0_seq1	<i>UGDH</i>	4.247935016	UDPglucose 6-dehydrogenase
comp11829_c0_seq1	<i>UGDH</i>	7.415677668	UDPglucose 6-dehydrogenase
comp13882_c0_seq1	<i>UGDH</i>	12.54341086	UDPglucose 6-dehydrogenase
comp2995_c0_seq1	<i>UGDH</i>	5.95883459	UDPglucose 6-dehydrogenase
comp9018_c0_seq1	<i>UGDH</i>	5.987751271	UDPglucose 6-dehydrogenase
comp6834_c0_seq1	<i>E5.1.3.6</i>	2.514345445	UDP-glucuronate 4-epimerase
comp7260_c0_seq1	<i>E5.1.3.6</i>	2.694759236	UDP-glucuronate 4-epimerase
comp7326_c0_seq1	<i>E5.1.3.6</i>	2.967354731	UDP-glucuronate 4-epimerase

RNA sequencing data identified 2864 genes with at least twofold higher transcript levels, and 1605 genes with at least twofold lower levels in drought stress conditions compared with the control (Fig. 4B,D). These genes are involved in multiple signaling pathways, particularly endocytosis, plant hormone signal transduction, phosphatidylinositol signaling system, starch and sucrose metabolism, cutin and wax biosynthesis, nitrogen metabolism biosynthesis of secondary metabolites, among others (Fig. 4C–F). The top 20 enriched pathways are described in Fig. 4D. Drought stress may affect hormone and cell wall biosynthesis signaling. We found 16 genes in ABA, ethylene, jasmonate, cytokinin, and auxin signal transduction (Table 1). The ABA receptor *PYR/PYL* (comp9009\_c0\_seq1) and *TF MYC2* (comp8652\_c0\_seq1) are two putative ABA downstream signaling genes, which also respond to drought stress [27]. We also identified four genes in cutin and wax biosynthesis pathways, and four genes involved in second messenger systems (Table 1). Homologue genes of *CER1* in *Oryza sativa* L. and *Arabidopsis thaliana* mediate cell wall synthesis, and respond to drought stress. *CER1* in taro was obviously increased. Drought stress caused taro extension by starch accumulation. We further selected starch biosynthesis-related genes. We found that six homologue genes were induced more than six times, which encoded trehalose 6-phosphate synthase/phosphatase. The transcript level of 5 Uridine Diphosphate (UDP)-glucose 6-dehydrogenase and 3 UDP-glucuronate 4-epimerase related genes was also increased (Table 2).

## 4. Discussion

### 4.1 Diversity of Starch Accumulation in Granule Size of Numerous Corm Taro

As starch accumulates in crops, starch granules display diverse morphological characteristics, such as shape and size, which further affect the physical and chemical

properties [28]. In *Oryza sativa* L., starch granules are large and polygonal with irregular shapes accompanied by some small spherical starch granules [28]. The diameter of rice starch granules is no more than 15  $\mu\text{m}$ . In *Triticum aestivum* L., starch granules are circular or elliptical in shape, with a few irregular particles [25]. A-type starch has a diameter of 25–35  $\mu\text{m}$ , and B-type starch has a diameter of only 2–8  $\mu\text{m}$ . Both Xiangsha taro and Longxiang taro are multiseed taro, which have similar growth characteristics in height, width, and weight. The taro starch basically presents an irregular polyhedron shape, with a smooth surface and plump particles, and generally no gap. The diameter of taro starch granules is about 1–4  $\mu\text{m}$  [29]. The main difference between the varieties is the size of the starch granules. The average starch granules size of Xiangsha taro is significantly larger than Longxiang taro starch in the same growth stage, and the grain size of Xiangsha taro changes with the growth period, showing a trend of gradual increase. Longxiang taro has no obvious increase trend at different times, and the grain size is always maintained at a constant level.

### 4.2 Drought Inhibits Starch Accumulation

The development of the taro plant is seriously inhibited under drought stress, especially seed taro formation and extension. Drought induces the root: shoot ratio and reduces total plant biomass loss. Nutrient efficiency, water use efficiency, chlorophyll content index, and nitrogen content could improve the photosynthesis rate. Trehalose plays a crucial role in starch biosynthesis by affecting the main raw materials supply [30]. The application of exogenous sugar has shown that trehalose functions as a key sugar signal during rice grain filling. Trehalose regulates the expression of genes related to sucrose conversion and starch synthesis, thereby promoting the conversion of sucrose to starch [31]. Transcriptome sequencing of drought-stressed taro corms has shown that trehalose 6-phosphate

synthase/phosphatase is upregulated, which might inhibit starch accumulation. The ratio of auxin and cytokinin is a key factor for shoot formation in rice and other crops [32]. Here, we also found that the transcript level of auxin and cytokinin-related genes were affected, as well as ABA. ABA is a stress-induced phytohormone, which accumulates in leaves to induce stomatal closure, preventing water loss through inhibition of transpiration [33]. Thus, a putative model is that drought stress inhibits starch accumulation and seed taro formation, as determined by the ratio of auxin and cytokinin. Further studies using transgenic taro are required to fully understand the mechanisms underlying taro growth.

## 5. Conclusions

This study showed that different crops have different characteristics of starch accumulation, especially starch granule size, which determine the use and processing of crop starch. Under drought stress, water use efficiency, nutrient efficiency, and photosynthetic efficiency lead to a reduction in total plant biomass, which might be due to sugar distribution and a hormone signaling pathway.

## Availability of Data and Materials

The authors confirm that the data supporting the findings of this study are available within the article. The datasets used and/or analyzed during the current study are available from the corresponding author upon reasonable request.

## Author Contributions

EZ, WJ, EA, and WL performed experiments and analyzed data. XY, YW and FX designed the experiment. FX supervised the experiment. EZ wrote and edited the manuscript. All authors have participated sufficiently in the work to take public responsibility for appropriate portions of the content and agreed to be accountable for all aspects of the work in ensuring that questions related to its accuracy or integrity. All authors read and approved the final manuscript. All authors contributed to editorial changes in the manuscript.

## Ethics Approval and Consent to Participate

The taro cultivars of Xiangsha and Longxiang in this study were provided by Lixiahe Agricultural Science Institute of Yangzhou, China.

## Acknowledgment

Not applicable.

## Funding

This study was supported by the Project funded by China Postdoctoral Science Foundation (2019M660130), a Project Funded by the Priority Academic Program Development of Jiangsu Higher Education Institutions (PAPD).

## Conflict of Interest

The authors declare no conflict of interest.

## References

- [1] FAO. FAOSTAT. Food and Agriculture Organization of the United Nations. 2019. Available at: <https://www.fao.org/faostat/en/#home> (Accessed: 10 December 2021).
- [2] Quach ML, Melton LD, Harris PJ, Burdon JN, Smith BG. Cell wall compositions of raw and cooked corms of taro, (*Colocasia esculenta*). *Journal of the Science of Food and Agriculture*. 2011; 81: 311–318.
- [3] Zhao L, Xu A, Zhang L, Yin Z, Wei C. Spatiotemporal accumulation and characteristics of starch in developing maize caryopses. *Plant Physiology and Biochemistry*. 2018; 130: 493–500.
- [4] Pérez S, Bertoft E. The molecular structures of starch components and their contribution to the architecture of starch granules: a comprehensive review. *Starch*. 2010; 62: 389–420.
- [5] Cruz de Carvalho MH. Drought stress and reactive oxygen species: Production, scavenging and signaling. *Plant Signaling & Behavior*. 2008; 3: 156–165.
- [6] Hanin M, Brini F, Ebel C, Toda Y, Takeda S, Masmoudi K. Plant dehydrins and stress tolerance: versatile proteins for complex mechanisms. *Plant Signaling & Behavior*. 2011; 6: 1503–1509.
- [7] Choudhury FK, Rivero RM, Blumwald E, Mittler R. Reactive oxygen species, abiotic stress and stress combination. *The Plant Journal: for Cell and Molecular Biology*. 2017; 90: 856–867.
- [8] Bacete L, Hamann T. The Role of Mechanoperception in Plant Cell Wall Integrity Maintenance. *Plants*. 2020; 9: 574.
- [9] Rui Y, Dinneny JR. A wall with integrity: surveillance and maintenance of the plant cell wall under stress. *The New Phytologist*. 2020; 225: 1428–1439.
- [10] Zhang X, Yang Z, Wu D, Yu F. RALF-FERONIA Signaling: Linking Plant Immune Response with Cell Growth. *Plant Communications*. 2020; 1: 100084.
- [11] Schuetz M, Benske A, Smith RA, Watanabe Y, Tobimatsu Y, Ralph J, *et al.* Laccases direct lignification in the discrete secondary cell wall domains of protoxylem. *Plant Physiology*. 2014; 166: 798–807.
- [12] Bidhendi AJ, Chebli Y, Geitmann A. Fluorescence visualization of cellulose and pectin in the primary plant cell wall. *Journal of Microscopy*. 2020; 278: 164–181.
- [13] De Lorenzo G, Ferrari S, Giovannoni M, Mattei B, Cervone F. Cell wall traits that influence plant development, immunity, and bioconversion. *The Plant Journal: for Cell and Molecular Biology*. 2019; 97: 134–147.
- [14] Underwood W. The plant cell wall: a dynamic barrier against pathogen invasion. *Frontiers in Plant Science*. 2012; 3: 85.
- [15] Tang C, Xiong D, Fang Y, Tian C, Wang Y. The two-component response regulator VdSkn7 plays key roles in microsclerotial development, stress resistance and virulence of *Vectricillium dahliae*. *Fungal Genetics and Biology*. 2017; 108: 26–35.
- [16] Novaković L, Guo T, Bacic A, Sampathkumar A, Johnson KL. Hitting the Wall-Sensing and Signaling Pathways Involved in Plant Cell Wall Remodeling in Response to Abiotic Stress. *Plants*. 2018; 7: 89.
- [17] Zhu Y, Huang P, Guo P, Chong L, Yu G, Sun X, *et al.* CDK8 is associated with RAP2.6 and SnRK2.6 and positively modulates abscisic acid signaling and drought response in Arabidopsis. *The New Phytologist*. 2020; 228: 1573–1590.
- [18] Chen K, Li GJ, Bressan RA, Song CP, Zhu JK, Zhao Y. Abscisic acid dynamics, signaling, and functions in plants. *Journal of Integrative Plant Biology*. 2020; 62: 25–54.
- [19] Chen Q, Bai L, Wang W, Shi H, Ramón Botella J, Zhan Q, *et al.* COP1 promotes ABA-induced stomatal closure by modulating the abundance of ABI/HAB and AHG3 phosphatases. *The New*

- Phytologist. 2021; 229: 2035–2049.
- [20] Nakashima K, Yamaguchi-Shinozaki K. ABA signaling in stress-response and seed development. *Plant Cell Reports*. 2013; 32: 959–970.
- [21] Hou YJ, Zhu Y, Wang P, Zhao Y, Xie S, Batelli G, *et al.* Type One Protein Phosphatase 1 and Its Regulatory Protein Inhibitor 2 Negatively Regulate ABA Signaling. *PLoS Genetics*. 2016; 12: e1005835.
- [22] Chong L, Guo P, Zhu Y. Mediator Complex: A Pivotal Regulator of ABA Signaling Pathway and Abiotic Stress Response in Plants. *International Journal of Molecular Sciences*. 2020; 21: 7755.
- [23] Zhu JK. Abiotic Stress Signaling and Responses in Plants. *Cell*. 2016; 167: 313–324.
- [24] Gouveia CSS, Ganança JFT, Slaski J, Lebot V, Pinheiro de Carvalho MAA. Stable isotope natural abundances ( $\delta^{13}\text{C}$  and  $\delta^{15}\text{N}$ ) and carbon-water relations as drought stress mechanism response of taro (*Colocasia esculenta* L. Schott). *Journal of Plant Physiology*. 2019; 232: 100–106.
- [25] Yu X, Li B, Wang L, Chen X, Wang W, Wang Z, *et al.* Systematic Analysis of Pericarp Starch Accumulation and Degradation during Wheat Caryopsis Development. *PLoS ONE*. 2015; 10: e0138228.
- [26] Huang X, Zhang Y, Wang L, Dong X, Hu W, Jiang M, *et al.* *OsDOF11* Affects Nitrogen Metabolism by Sucrose Transport Signaling in Rice (*Oryza sativa* L.). *Frontiers in Plant Science*. 2021; 12: 703034.
- [27] Qiu J, Xie J, Chen Y, Shen Z, Shi H, Naqvi NI, *et al.* Warm temperature compromises JA-regulated basal resistance to enhance *Magnaporthe oryzae* infection in rice. *Molecular Plant*. 2022; 15: 723–739.
- [28] Chen X, Chen M, Lin G, Yang Y, Yu X, Wu Y, *et al.* Structural development and physicochemical properties of starch in caryopsis of super rice with different types of panicle. *BMC Plant Biology*. 2019; 19: 482.
- [29] Yu X, Zhang Y, Ran L, Lu W, Zhang E, Xiong F. Accumulation and physicochemical properties of starch in relation to eating quality in different parts of taro (*Colocasia esculenta*) corm. *International Journal of Biological Macromolecules*. 2022; 194: 924–932.
- [30] Min X, Xu H, Huang F, Wei Y, Lin W, Zhang Z. GC-MS-based metabolite profiling of key differential metabolites between superior and inferior spikelets of rice during the grain filling stage. *BMC Plant Biology*. 2021; 21: 439.
- [31] Kurepa J, Smalle JA. Auxin/Cytokinin Antagonistic Control of the Shoot/Root Growth Ratio and Its Relevance for Adaptation to Drought and Nutrient Deficiency Stresses. *International Journal of Molecular Sciences*. 2022; 23: 1933.
- [32] Gouveia CSS, Ganança JFT, de Nóbrega HGM, de Freitas JGR, Lebot V, Pinheiro de Carvalho MAA. Phenotypic flexibility and drought avoidance in taro (*Colocasia esculenta* (L.) Schott). *Emirates Journal of Food and Agriculture*. 2020; 32: 150–159.
- [33] Gouveia CSS, Ganança JFT, Slaski J, Lebot V, Pinheiro de Carvalho MAA. Involvement of abscisic acid and other stress indicators in taro (*Colocasia esculenta* (L.) Schott) response to drought conditions. *Acta Physiologiae Plantarum*. 2020; 42: 1–11.